0026-895X/04/6501-56–67$20.00
MOLECULAR PHARMACOLOGY
Copyright © 2004 The American Society for Pharmacology and Experimental Therapeutics
Mol Pharmacol 65:56–67, 2004

Vol. 65, No. 1
2877/1118435
Printed in U.S.A.

Hydroxy Metabolites of the Alzheimer's Drug Candidate 3-[(2,4-Dimethoxy)Benzylidene]-Anabaseine Dihydrochloride (GTS-21): Their Molecular Properties, Interactions with Brain Nicotinic Receptors, and Brain Penetration

William R. Kem, Vladimir M. Mahnir,[1] Laszlo Prokai, Roger L. Papke, Xuefang Cao, Susan LeFrancois, Kristin Wildeboer, Katalin Prokai-Tatrai, Julia Porter-Papke, and Ferenc Soti

Department of Pharmacology and Therapeutics, College of Medicine (W.R.K.,V.M.M., R.L.P., X.C., S.L.F., K.W., K.P.-T., J.P.-P., F.S.) and Department of Medicinal Chemistry, College of Pharmacy (L.P.), University of Florida, Gainesville, Florida

Received August 4, 2003; accepted September 26, 2003

This article is available online at http://molpharm.aspetjournals.org

ABSTRACT

3-[(2,4-Dimethoxy)benzylidene]-anabaseine dihydrochloride (DMXBA; GTS-21), an Alzheimer's drug candidate, selectively stimulates α7 nicotinic acetylcholine receptors. It rapidly enters the brain after oral administration and enhances cognitive behavior. Less than 1% of orally administered DMXBA is recovered in the urine. We report the identification and characterization of the major phase I metabolites of this drug candidate. Three hydroxy metabolites were generated in vitro by hepatic microsomal *O*-dealkylation of the two methoxy substituents on the benzylidene ring. They were also found in plasma of rats after oral administration, but at significantly lower concentrations relative to the parent compound. The metabolites displayed similar binding affinities and partial agonist potencies at rat brain α7 receptors. However, each displayed a higher efficacy than DMXBA for stimulating rat and human α7 receptors. Like DMXBA, the metabolites were weak antagonists at $\alpha_4\beta_2$ receptors. The predicted conformations of the metabolites were nearly identical with that of DMXBA. Ionization of the tetrahydropyridyl nitrogen was essential for high-affinity binding of DMXBA to the α7 receptor. The hydroxy metabolites were much more polar than DMXBA, derived from their experimentally estimated octanol/water partition coefficients, and they entered the brain much less readily than DMXBA. Their contributions to the behavioral effects of orally administered DMXBA, if any, would probably be very small during short-term administration. Benzylidene anabaseines pharmacologically similar to the hydroxy metabolites, but which enter the brain more readily, may provide greater stimulation of α7 receptors in the whole organism.

Although nicotinic cholinergic receptors (nAChRs) in the brain have long been recognized as being important in mediating the euphoric effects of nicotine, they attracted additional interest when significant nAChR deficits, later identified as primarily of the $\alpha_4\beta_2$ receptor subtype, were discovered in postmortem brain samples from patients with Alzheimer's disease (Sabbagh et al., 1998). Mammalian nAChRs are pentameric ligand-gated ion channels that, upon activation, allow the movement of cations including calcium across the cell membrane. Besides causing membrane depolarization, nAChR (especially the α7 type)-mediated influx of calcium into the cell stimulates several signal transduction pathways (Kihara et al., 2001; Dajas-Bailador et al., 2002). A variety of nAChR subtypes are now known to be present in the mammalian brain. The two most abundant brain

This research was partially supported by Taiho Pharmaceutical Company, Ltd., Tokyo and Tokushima, Japan (to W.K. and R.P.), National Institute of Mental Health grant R01-MH6142 (to R.F. and W.K.), Florida Biomedical Research Program grant BM013 (to W.K. and L.P.), and National Institutes of Health grant NS32888-02 (to R.P.).

Initial report of the DMXBA metabolites: Kem WR, Mahnir VM, Lin B, and Prokai-Tatrai K (1996) Two primary GTS-21 metabolites are potent partial agonists at α7 nicotinic receptors expressed in the *Xenopus* oocyte. *Soc Neurosci* **22:**268.

[1]Current address: Bachem California Inc., Torrance, CA 90505.

ABBREVIATIONS: nAChR, nicotinic acetylcholine receptor; FAB, fast-atom bombardment; MS, mass spectrometry; LC, liquid chromatography; LC/MS, liquid chromatography/mass spectrometry; HPLC, high-performance liquid chromatography; ACh, acetylcholine; BTX, α-bungarotoxin; DMXBA, 3-[(2,4-dimethoxy)benzylidene]-anabaseine dihydrochloride; 4-OH-MBA, 3-[(4-hydroxy-2-methoxy)benzylidene]-anabaseine dihydrochloride; 2-OH-MBA, 3-[(2-hydroxy-4-methoxy)benzylidene]-anabaseine dihydrochloride; 2,4-OH-BA, 3-[(2,4-dihydroxy)benzylidene]-anabaseine dihydrochloride; GTS-83, 3-[3,4-(1,2-ethylenedioxy)benzylidene]-anabaseine; 2,4-DiOH-BA, 3-[(2,4-dihydroxy)benzylidene]-anabaseine; Br:Bl, brain-to-blood; 5-HT, 5-hydroxytryptamine; MOPS, 4-morpholinepropanesulfonic acid; $P_{octanol/water}$, octanol/water partition coefficient.

nAChRs are the heteromeric $\alpha_4\beta_2$ and homomeric α7 subtypes. The former contributes >90% of the high-affinity binding sites for nicotine in the rat brain (Flores et al., 1992). The low-nicotine-affinity α7 nAChR is recognized by its nanomolar affinity for α-bungarotoxin (Marks and Collins, 1982). These two widely distributed brain nAChR subtypes occur in cortical and hippocampal neurons involved in cognitive functions. Other brain, autonomic ganglia, and skeletal muscle nAChRs are composed of different subunit combinations (Lindstrom, 1996; Champtiaux et al., 2002).

Decreases in the low-nicotine-affinity α7-type receptors were very small in the postmortem brains of patients with Alzheimer's disease (Martin-Ruiz et al., 1999). However, it has been suggested that the α7 nAChR is an important target for β-amyloid–mediated neurotoxicity (Wang et al., 2000). β-Amyloid$_{1-42}$ activation of α7 receptors expressed in the *Xenopus laevis* oocyte was prevented by two α7 ligands, the antagonist methyllycaconitine and a metabolite of DMXBA, which is a focus of this article (Dineley et al., 2002). α7 Receptor agonists enhance cognition and auditory-gating processes and thus are attractive drug candidates for the treatment of senile dementias and schizophrenia (Freedman et al., 1996; Stevens et al., 1998; Kem, 2000).

Anabaseine is an animal toxin that, like nicotine, stimulates all nAChRs (Kem et al., 1997). DMXBA (code name GTS-21) (Fig. 3), a synthetic benzylidene derivative of anabaseine, selectively stimulates α7 subunit-containing nAChRs (de Fiebre et al., 1995; Meyer et al., 1998). Its efficacy (maximum effect) for activating the rat α7 receptor is approximately half that observed for ACh and anabaseine, which are full agonists. DMXBA efficacy at the human α7 receptor is only approximately 20% of the ACh maximal response (Meyer et al., 1998). DMXBA enhances cognitive behavior in aging and nucleus basalis-lesioned mammals, including monkeys (Woodruff-Pak et al., 1994; Arendash et al., 1995; Briggs et al., 1997; Buccafusco and Terry, 2000). It also displays neuroprotective properties (Martin et al., 1994; Kihara et al., 1997; Shimohama et al., 1998). DMXBA did not display significant human toxicity in a phase I clinical trial (Kitagawa et al., 2003).

Initial pharmacokinetic analyses indicated that orally administered DMXBA is rapidly metabolized (Mahnir et al., 1998). The major goal of the present study was to compare the molecular and pharmacological properties of the primary metabolites with DMXBA.

Materials and Methods

Materials. Radioligands [^{3}H]cytisine and [^{125}I]BTX were purchased from PerkinElmer Life and Analytical Sciences (Boston, MA). Reagents for chemical syntheses, NADPH, and various solvents were purchased from Sigma-Aldrich (St. Louis, MO). Commonly used chemicals and solvents were purchased from Fisher Chemical Co. (Orlando, FL). Bicinchoninic acid protein assay reagent was obtained from Pierce Chemical (Rockford, IL). Recombinant rat cytochrome P450 supersomes 1A1, 1A2, and 3A2 expressed in baculovirus insect cells were purchased from BD Gentest (Woburn, MA). Neuronal nAChR subunit cDNAs were graciously provided by Dr. James Boulter (Salk Institute, San Diego, CA) and Dr. Jon Lindstrom (University of Pennsylvania, Philadelphia, PA). RNA transcription kits were purchased from Ambion (Austin, TX). Collagenase A was purchased from Roche Diagnostics (Indianapolis, IN). Male Sprague-Dawley rats (200–250 g) were purchased from Charles River Breeding Laboratories (Raleigh, NC) and Harlan (Indianapolis, IN).

Synthesis and Chemical Analysis of DMXBA and Metabolites. All of these compounds were synthesized by reaction of anabaseine dihydrochloride with the appropriate benzaldehyde (Kem, 1971; Zoltewicz et al., 1993). Melting point (m.p.) values are uncorrected. Elemental analyses were supplied by Atlantic Microlabs, Inc. (Norcross, GA). ^{1}H NMR chemical shifts (in ppm) were recorded in dimethyl sulfoxide-d_6 using tetramethylsilane as a reference on a VXR 300 spectrometer (Varian, Inc., Palo Alto, CA). Mass spectra of the synthetic compounds were recorded on an MS80RFA spectrometer (Kratos Analytical, Manchester, UK). Fast atom bombardment (FAB) analyses used an 8-kV xenon beam and 3-nitrobenzyl alcohol as a matrix. Accurate mass measurements were carried out after direct introduction and 70-electron volt electron ionization at a nominal mass resolution of 10,000 with a perfluorokerosene internal standard.

Synthesis of DMXBA was initiated by dissolving anabaseine dihydrochloride (6.0 g, 0.024 mol) and 2,4-dimethoxybenzaldehyde (9.0 g, 0.054 mol) in 350 ml of ethanol containing approximately 20 drops of concentrated HCl. The solution was stirred at 75°C overnight. After cooling, 1.2 g of product was collected by filtration. Ether (approximately 800 ml) was added to the mother liquor until no more precipitate appeared. The combined solids were dissolved in methanol and precipitated with ether. This procedure was repeated several times. The product (8.1 g) was obtained as a yellow solid in 89% yield, m.p. 216 to 217°C (dec). Analytical calculation for $C_{19}H_{20}N_2O_2 \times$ 2HCl (mol. wt. 381): C, 59.85; H, 5.82; N, 7.35. Found: C, 59.54; H, 5.89; N, 7.41. ^{1}H NMR: 8.94 (d, J = 1.5 Hz, H2′), 8.92 (dd, J = 4.9 and 1.7 Hz, H6′), 8.22 (dd, J = 8.6 and 1.9 Hz, H4′), 7.79 (dd, J = 7.9 and 5.1 Hz, H5′), 7.60 (d, J = 8.8 Hz, H13), 7.31 (s, H10), 6.70 (dd, J = 8.8 and 2.4 Hz, H12), 6.65 (s, H7), 3.85 (s, OMe), 3.80 (t, J = 5.7 Hz, H6), 3.72 (s, OMe), 2.92 (t, J = 5.7 Hz, H4), and 2.02 (qn, J = 5.6 Hz, H5). High-resolution electron ionization-MS: 308.1525 expected, 308.1557 calculated.

4-OH-MBA was prepared as a yellow hygroscopic solid in 85% yield from anabaseine hydrochloride and 4-hydroxy-2-methoxybenzaldehyde using the same procedure as described above, m.p. 215 to 219°C (dec). Analytical calculation for $C_{18}H_{18}N_2O_2 \times$ 2HCl (mol. wt. 367): C, 58.87; H, 5.49; N, 7.63. Found: C, 58.40; H, 5.79; N, 6.33. ^{1}H NMR: 8.92 (d, J = 5.0 Hz, H6′), 8.87 (d, J = 1.8 Hz, H2′), 8.17 (d, J = 8.0 Hz, H4′), 7.76 (dd, J = 8.0 and 5.0 Hz, H5′), 7.55 (d, J = 8.8 Hz, H13), 7.34 (s, H7), 6.59 (d, J = 10.7 Hz, H12), 6.50 (d, J = 2.3 Hz, H10), 3.78 (tr, J = 10.7 Hz, H6), 3.65 (s, OMe), 2.93 (tr, J = 11.1 Hz, H4), and 2.03(tr, J = 10.5 Hz, H5). FAB-MS: m/z 295 $(M+H)^+$.

2-OH-MBA was obtained as a yellow hygroscopic solid in 86% yield from anabaseine dihydrochloride and 2-hydroxy-4-methoxybenzaldehyde, m.p. 215 to 219°C (dec). Analytic calculation for $C_{18}H_{18}N_2O_2 \times$ 2HCl (mol. wt. 367): C, 58.87; H, 5.49; N, 7.63. Found: C, 58.59; H, 5.76; N, 7.47. ^{1}H NMR: 8.82 (s, H2′), 8.80 (bd, J = 4.9 Hz, H6′), 8.10 (dd, J = 7.5 and 1.5 Hz, H4′), 7.71 (dd, J = 7.5 and 4.5 Hz, H5′), 7.59 (d, J = 9.0 Hz, H13), 7.41 (s, H7), 6.58 (d, J = 8.6 Hz, H12), 6.52 (s, H10), 3.77 (s, OMe), 3.61 (tr, J = 5.5 Hz, H6), 2.94 (tr, J = 5.2 Hz, H4), and 2.03 (qn, J = 5.1 Hz, H5). FAB-MS: m/z 295 $(M+H)^+$.

2,4-OH-BA was synthesized essentially as described above, but the acid catalyst was omitted because of the acid instability of 2,4-dihydroxybenzaldehyde. The product was obtained in 50% yield as a very hygroscopic solid, m.p. 256 to 259°C (dec). Analytical calculation for $C_{17}H_{16}N_2O_2 \times$ 2HCl (mol. wt. 353): C, 57.80; H, 5.14; N, 7.93. Found: C, 56.71; H, 5.26; N, 7.70. ^{1}H NMR: 8.86 (bd, J = 5.1 Hz, H6′), 8.79 (bs, H2′), 8.05 (d, J = 7.9 Hz, H4′), 7.66 (dd, J = 7.7 and 4.9 Hz, H5′), 7.51(d, J = 9.0 Hz, H13), 7.42 (s, H7), 6.39 (broad, H12 and N^+H), 6.32 (s, H10), 3.78 (tr, J = 5.4 Hz, H6), 2.92 (tr, J = 5.8 Hz, H4), and 2.02 (qn, J = 5.1 Hz, H5). FAB-MS: m/z 281 $(M+H)^+$.

In Vitro Hepatic Biotransformation Experiments. For the initial LC and LC/MS identification of the DMXBA hepatic microsome metabolites, 500 μM DMXBA was incubated for 16 h at 37°C in 500 μl of saline containing 500 μg (fresh weight) of a rat microsomal membrane pellet prepared according to the procedure of James and Little (1983) to achieve nearly complete phase I biotransformation.

The incubation medium in open test tubes contained 2.0 mM NADPH. Microsomal biotransformations were terminated by 4 min of heat denaturation at 99°C. After deproteination by adding 2 volumes of acetonitrile and centrifuging for 10 min at 15,000*g*, the resulting supernatant was rotary-evaporated at 40°C to remove all solvents. The crude metabolite sample was then redissolved in 500 μl of 0.1% trifluoroacetic acid, centrifuged, and then passed through a 0.45-μm nylon filter before being resolved by gradient C18 reversed-phase HPLC (Fig. 1A shows the conditions).

For thermospray LC/MS identification of the microsomal metabolites, a 4.6-mm i.d. × 15-cm Supelcosil LC-ABZ column (Supelco, Bellefonte, PA), protected with a Supelguard cartridge, was eluted with an isocratic mobile phase of 15% acetonitrile in 0.05 M aqueous ammonium acetate (pH was set to 4.5 with acetic acid). Mass spectral identification of the LC-resolved metabolites was carried out on a Vestec model 201 quadrupole instrument (Applied Biosystems, Foster City, CA). Mass scale calibration was done by using the positive ions of polyethylene oxide oligomers (PEG 300) produced under pure thermospray conditions without discharge. Total ion current and mass chromatograms were reconstructed from the stored mass spectra.

To determine the kinetic parameters governing the biotransformation of DMXBA by rat hepatic microsomes, 500-μl aliquots containing 500 μg of fresh weight of rat microsomal membrane pellet (prepared as described above) were incubated at 37°C with different concentrations of DMXBA (or related compounds) in open test tubes containing 2.0 mM NADPH for variable periods from 5 min to 1 h. Biotransformation was terminated by heat denaturation as described previously. Afterward, 200 ng of the internal standard GTS-83 was added to each sample before it was filtered (Costar 0.45 μm of nylon) and centrifuged before HPLC.

After the initial identification and synthesis of the metabolites, a standardized HPLC assay was developed to measure their concentrations in various fluids and tissues. Using a 50 mM ammonium acetate-buffered (pH 4.5) acetonitrile gradient (5–60%) at a flow rate of 2.0 ml/min over 15 min, the compounds eluted separately from an ODS C18 analytical column as follows: 2,4-DiOH-BA (3.8 min), 4-OH-MBA (5.3 min), 2-OH-MBA (6.2 min), internal standard GTX-83 (7.4 min), and DMXBA (8.0 min). At a wavelength of 400 nm, all were readily resolved and measured at nanomole levels.

Whole Animal Biotransformation Experiments. To determine the rates of elimination of orally administered DMXBA or a synthesized hydroxy metabolite, male Sprague-Dawley rats were cannulated in the right jugular vein to permit serial time-sampling of blood. Each rat daily received sodium heparin (50 units) to maintain cannula patency and prevent coagulation of plasma samples. DMXBA or one of its synthetically prepared metabolites was administered orally by gavage at a dose of 20 mg/kg. Blood samples (100–300 μl) were drawn 0.5, 1, 2, 4, 6, and 8 h after oral administration; smaller volumes sufficed for the initial times. Each blood sample was replaced intravenously with an equal volume of sterile saline. After centrifugation of each blood sample, 200 ng of GTS-83 was added to each milliliter of separated plasma, which was then subjected to solid-phase extraction on a Bond Elut column (Varian Inc., Palo Alto, CA), as described by Azuma et al. (1996). The resulting sample was centrifuged through a 0.45-μm nylon filter before automatic injection into a Supelcosil (Ultrasphere ODS 5 μm 4.6 × 25 cm) C18 column connected to a Gold Nouveau HPLC (all from Beckman Coulter, Fullerton, CA). Control experiments involving the simultaneous addition of DMXBA or individual metabolites and GTS-83 to untreated rat plasma indicated that extraction efficiencies of all of these compounds exceeded 95%.

DMXBA and Metabolite Brain: Blood Ratio Determinations. To measure brain and whole-blood concentrations of DMXBA and its metabolites, rats were administered four consecutive 20 mg/kg i.p. doses of a compound (DMXBA, 4-OH-MBA, 2-OH-MBA, or 2,4-DiOH-BA) at 2-h intervals. This protocol was selected to attain a near steady-state plasma concentration for each administered compound, assuming a plasma half-life of approximately 2 h (Fig. 2B). One hour after the last injection, each rat was decapitated, and its trunk blood and brain were removed for compound extraction and HPLC determination. Brain and blood samples were frozen at −20°C before extraction. The thawed brain was homogenized with 3 v/g fresh weight of ice-cold 0.9% NaCl. DMXBA and its metabolites were

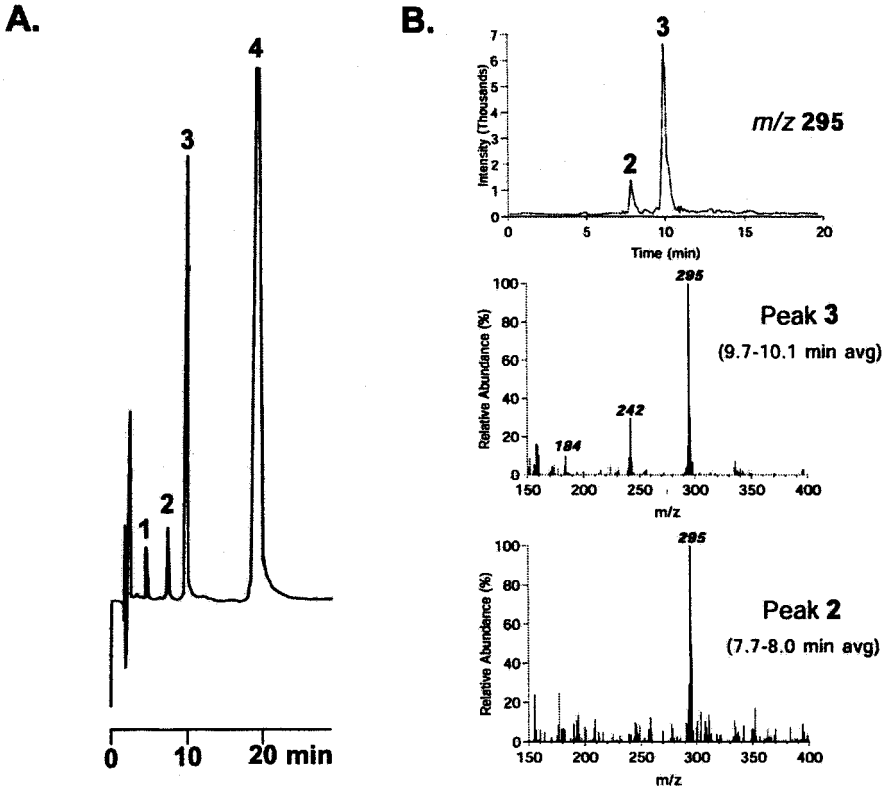

Fig. 1. HPLC separation of primary in vitro metabolites of DMXBA. A, for identification of the metabolites, a Supelcosil LC-ABZ column was isocratically eluted with 15% acetonitrile in 0.05 M aqueous ammonium acetate buffer, pH 4.5, at 1.0 ml/min over a period of 30 min. The compounds were detected at a wavelength of 400 nm. Taken from thermospray LC/MS analysis (B) and coelution with synthetic compounds, the DMXBA metabolites were assigned as follows: compound 1: 2,4-DiOH-BA; compound 2: 4-OH-MBA; and compound 3: 2-OH-MBA. Peak 4 is the internal standard GTS-83. DMXBA was absent after the 16-h incubation period. B, thermospray LC/MS mass chromatograms (m/z 295) and thermospray mass spectra of the two protonated monohydroxy in vitro rat liver microsomal metabolites of DMXBA. HPLC conditions were identical with those indicated in A, except for the use of a 100-μl loop in the injector valve. The thermospray probe receiving the column effluent was adjusted to a temperature of 150°C. The MS tip, source, and vapor temperatures were 325, 300, and 280°C, respectively. During analysis, discharge conditions (300-μA current) were maintained in the source by a 1000-V electrode. The analyzer, set for transmitting positive ions, was scanned repetitively from m/z 150 to 800 in 6-s cycles under the control of a Teknivent (St. Louis, MO) Vector/two data system and mass spectra were stored for latter processing. Positive-ion mass spectra were recorded under discharge ionization.

extracted from brain homogenate and whole-blood samples by either of two methods. GTS-83 (200 ng) was added to each 500 μl of blood or brain homogenate before proceeding with either solvent extraction protocol. Initially, we used a slight modification of a liquid-phase extraction method (Matuszewski et al., 1994), which included the removal of an initial brain trichloroacetic acid precipitate by centrifugation. Later, after many attempts to improve extraction efficiencies (20–35%) of DMXBA and its hydroxy metabolites, we resorted to a simpler acetone-extraction protocol, which gave similar results. In this protocol, 3.0 ml of acetone, 0.5 ml of water, and 200 ng of GTS-83 were added per 500 μl of tissue homogenate or plasma sample. The resulting solution was vortexed and then placed on a shaker for 1 h at room temperature in the dark. After removal of organic solvents under vacuum, the dried samples were dissolved in starting HPLC buffer to a total volume of 500 μl, vortexed for 10 s, and filtered before HPLC determinations.

Brain Nicotinic Receptor Radioligand Binding Assays. After decapitation, washed whole rat brain membranes (200 μg of protein) were prepared according to the method used by Marks and Collins (1982). Before use, the washed membranes were resuspended in 500-μl receptor binding assay saline (pH 7.40) consisting of 120 mM NaCl, 5 mM KCl, 2 mM $CaCl_2$, 1 mM $MgCl_2$ and 50 mM Tris-HCl. [^{3}H]Cytisine (35 Ci/mmol)-binding displacement experiments were performed essentially according to Flores et al. (1992), except that the incubation time was increased to 4 h at 0 to 4°C to ensure equilibrium during the competition binding assay. Binding of ^{125}I-BTX (136 Ci/mmol) was performed at 37°C for 3 h; the saline solution mentioned above also contained 2 mg/ml bovine serum albumin. Nonspecific binding of each radioligand was measured in the presence of 1.0 mM nicotine (Marks and Collins, 1982). After incubation, membranes with bound radioligand were collected on Whatman GF/C glass fiber filters presoaked for 45 min in 0.5% polyethylenimine and washed three times with 3.0 ml of ice-cold buffer by vacuum filtration on a harvester (Brandel, Gaithersburg, MD). Bound [^{3}H]cytisine was measured in a liquid scintillation counter, whereas [^{125}I]BTX was measured with use of a Biogamma counter (both from Beckman Coulter). Binding data were analyzed using Prism software (GraphPad Software Inc., San Diego, CA). All K_i values were calculated from the Cheng-Prusoff equation, using a K_d value for each radioligand that had been experimentally determined under conditions identical with those of the displacement experiments.

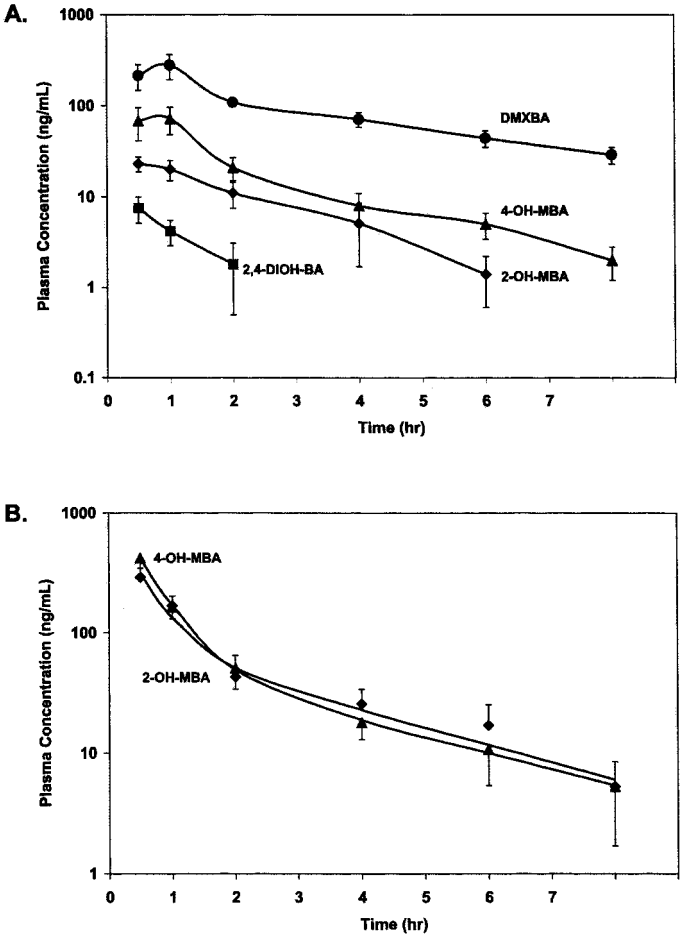

Fig. 2. Plasma concentrations of DMXBA and its primary metabolites, as determined by HPLC. A, concentrations of DMXBA and its metabolites after oral administration (20 mg/kg) of DMXBA to male Sprague-Dawley rats. B, concentrations of 4-OH-MBA and 2-OH-MBA resulting from their oral administration (20 mg/kg) to male Sprague-Dawley rats. The plasma concentrations in B were found to fit a two-compartment pharmacokinetic model [c = L·exp(−α·) + tM·(exp(−β·)] (Gibaldi and Perrier, 1982) with parameters as follows: For 4-OH-MBA, L = 1044.1 ng/ml, α = 2.136 h^{-1}, M = 64.47 ng/ml, β = 0.310 h^{-1}, elimination half-life (ln2/β) = 2.24 h. For 2-OH-MBA, A = 780.0 ng/ml, α = 2.381 h^{-1}, B = 86.42 ng/ml, β = 0.333 h^{-1}, elimination half-life = 2.08 h.

Pharmacological Effects of DMXBA Metabolites upon Rodent and Human Nicotinic Receptors Expressed in *X. laevis* Oocytes. The experimental protocols for obtaining concentration-response curves for the two metabolites, 2-OH-MBA and 2,4-DiOH-BA, were identical with those described previously for 4-OH-MBA and DMXBA (Papke and Porter-Papke, 2002). Peak currents were measured for responses of $\alpha_4\beta_2$ receptors to agonist application, because desensitization of this receptor subtype was slow enough not to affect the concentration-response relation measured in this manner. Currents resulting from agonist application to the more rapidly desensitizing α7 receptors were integrated over a period of 90 s after application commenced. To compare data obtained from different oocytes, a standard response normalization procedure was used. Agonist responses of a particular oocyte were always normalized relative to its response to a standard ACh control. Before actual measurements of agonist properties, several ACh pulses separated by 5-min intervals were applied until the responses of the oocyte to ACh became steady. After washing for 5 min, the peak current response to the test compound was measured. After another 5-min washing period, ACh was again applied to measure the residual responsiveness of the receptors to ACh after exposure to the test substance. The concentration-response data were fitted with a modified Hill equation, $I = I_{max}$ [agonist]^{nH}/([agonist]^{nH} + EC_{50}), to estimate apparent efficacy (normalized maximal response) and EC_{50}.

pK_a Measurements. The pK_a of the most basic (imine) nitrogen in each compound was determined by analysis of the pH dependence of its electronic absorbance spectrum, recorded at room temperature (25°C) in the presence of 150 mM NaCl. Approximately 15 (range, 12–17) absorbance points, corresponding to different pH values in the titration region, were analyzed with use of the Enzfitter software (Elsevier-Biosoft, Cambridge, UK) to estimate each pK_a value. Absorbance changes at more alkaline pH levels, reflecting ionization of the aromatic hydroxyls, were also used to obtain pK_a values for these groups.

Octanol-Water Partition Coefficient Determinations. These were determined for each compound by HPLC analysis of the aqueous and organic phases after overnight equilibration on a gentle shaker at room temperature. The octanol and saline phases were allowed to equilibrate before use. Each compound (approximately 1 mg) was initially dissolved in 5.0 ml of aqueous phase containing 150 mM NaCl and 10 mM sodium phosphate buffer, pH 7.4, and then 5.0 ml of saline-octanol phase was added. After centrifugation, the entire octanol phase was carefully removed with a Pasteur pipette. The compound present in this phase was first back-extracted into three consecutive new 5.0-ml aqueous phases containing 150 mM NaCl (adjusted to pH < 2 with glacial acetic acid to drastically reduce solubility in octanol). Partition coefficient estimates were means of at least four separate experiments.

Plasma Protein Binding. To determine the free (unbound) fraction of each compound in whole plasma, 5 and 20 μg/ml compound were incubated in 1.0-ml aliquots of rat plasma at 37°C for 1 h. Each plasma sample was placed in a Centrifree ultrafiltration unit (Millipore Corporation, Bedford, MA)and centrifuged at 4,000*g* for 5 min to obtain approximately 200 μl of ultrafiltrate. The ultrafiltrate and resulting plasma samples were extracted with use of the Bond Elut method described by Azuma et al. (1996). GTS-83 (200 ng) was added to each sample after ultrafiltration. Concentrations of the compounds in these two phases were then determined by HPLC.

Molecular Modeling of Preferred Conformations. Molecular models for DMXBA and its putative metabolites were calculated using a semiempirical quantum mechanical method (PM5 parameters). Geometry optimizations were done by using a conductor-like screening (COSMO) model for solvation in water (Klamt and Shuurmann, 1993). CAChe Worksystem Pro (version 5.04; Fujitsu America, Inc., Beaverton, OR), a personal computer-based molecular-modeling program, was used in these computations.

Prediction of Partitioning Properties of DMXBA and Its Metabolites. The octanol/water partition coefficient ($P_{octanol/water}$) was calculated with use of an atom-fragment method (Viswanadhan et al., 1989) using CompuDrug software available online at http://www.compudrug.com (CompuDrug Inc., San Francisco, CA). The brain-to-blood (Br:Bl) concentration ratio was predicted from an AM1 semiempirical quantum chemical model (without COSMO solvation) of each compound using the equation (Brewster et al., 1996) $log\ Br{:}Bl = -0.2358D - 0.3485n_{ONH} + 4.062Q_N{}^4 + 0.6933$, where D is the AM1-calculated dipole moment, n_{ONH} is the number of O-H and N-H groups on the molecule, and Q_N is the sum of formal charges on the nitrogen atoms (two for each compound).

Results

In Vitro Hepatic Microsomal Metabolism. The three rings of DMXBA provide several potential sites for phase I biotransformation. However, because several major hepatic cytochromes P450 are known to catalyze the oxidative *O*-dealkylation of a variety of substrates, the two methoxy substituents on the benzylidene ring seemed particularly vulnerable. Indeed, incubation of a high concentration (500 μM) of DMXBA with rat hepatic microsomes yielded three new compounds, labeled according to their order of elution, which were readily resolved and detected by reversed-phase HPLC (Fig. 1A). Thermospray LC/MS analysis (Fig. 1B) revealed that the two major metabolites, corresponding to peaks 2 and 3 in Fig. 1B, had identical molecular ions ($[M+H]^+$) of m/z 295, as expected for a monohydroxy metabolite of DMXBA. The much smaller peak 1 displayed a molecular ion ($[M+H]^+$) of m/z 281 (data not shown), as expected for 2,4-DiOH-BA, the dihydroxy metabolite of DMXBA. The HPLC retention times and mass spectra of the synthesized putative metabolites described under *Materials and Methods* were found to match those of the microsomal metabolites: peak 1 was 2,4-DiOH-BA, peak 2 was 4-OH-MBA, and peak 3 was 2-OH-MBA. Peak 4 was the internal standard GTS-83; the parent compound DMXBA was no longer detectable after the 16-h incubation period.

We obtained typical hyperbolic substrate-concentration-versus-initial-reaction velocity curves for cytochrome P450-mediated biotransformations of DMXBA into its two monohydroxy metabolites from which the Michaelis-Menten kinetic parameters were calculated by computer fitting (Table 1). The K_m for the production of 4-OH-MBA was approximately 6-fold lower than the K_m for generation of 2-OH-MBA. However, the microsomal V_{max} for the generation of 2-OH-MBA was higher (Table 1). At relatively low DMXBA substrate concentrations, the predominant metabolite was 4-OH-MBA, whereas at higher concentrations, production of 2-OH-MBA dominated. Rat liver microsomal *O*-demethylation of 3-[(2-methoxy)benzylidene]-anabaseine, an analog prepared to observe *ortho*-demethylation in the absence of *para*-demethylation, yielded a similar V_{max} for 2-OH-BA production but a K_m value that was a 3-fold lower concentration than for biotransformation of DMXBA to 2-OH-MBA.

TABLE 1

Biotransformation of DMXBA by rat cytochrome P450 preparations (Michaelis-Menten kinetic properties for the two alternative pathways of *O*-demethylation shown in Fig. 3)

Tubes containing rat microsomes contained 1000 μg of membrane protein, whereas tubes containing recombinant cytochrome P450 supersomes 1A1, 1A2, and 3A2 contained 15, 27, and 45 μg of protein, respectively. Standard errors are shown.

Biotransformation	K_m	V_{max}
	μM	$\mu mol/mg\ protein\text{-}min$
Rat liver microsomes		
DMXBA → 4-OH-MBA	2.98 ± 0.58	34.4 ± 1.98
DMXBA → 2-OH-MBA	16.7 ± 1.84	81.3 ± 3.87
2-OH -MBA → 2,4-DiOH-BA	6.61 ± 2.46	20.6 ± 2.73
2-MeO-BA[a] → 2-OH-BA	5.72 ± 0.67	91.7 ± 3.74
Recombinant rat cytochromes P450		
1A1: DMXBA → 4-OH-MBA	0.206 ± 0.042	7670 ± 199
1A2: DMXBA → 4-OH-MBA	0.525 ± 0.19	2120 ± 137
3A2: DMXBA → 4-OH-MBA	18.1 ± 2.27	1830 ± 109
DMXBA → 2-OH-MBA	21.1 ± 1.04	1180 ± 29.3

[a] 2-MeO-BA is an analog of DMXBA that lacks the 4-OH group.

The two monohydroxy metabolites of DMXBA differed in their ability to undergo further metabolic oxidation. Separate incubations of a wide range of concentrations of 4-OH-MBA and 2-OH-MBA with rat liver microsomes for periods as long as 60 min revealed that only 2-OH-MBA was significantly converted to 2,4-DiOH-BA under these in vitro conditions. We also noticed that during storage of the rat microsomes at −85°C, their ability to produce the 2-OH-MBA disappeared over a period of a few weeks, whereas the ability to generate 4-OH-MBA from DMXBA was much less labile.

Biotransformation of DMXBA was catalyzed by three recombinant rat cytochromes P450 (Table 1). Both cytochromes 1A1 and 1A2 catalyzed the formation of 4-OH-MBA, whereas formation of 2-OH-MBA was not detected. Cytochrome 3A2 catalyzed the formation of both monohydroxy products in a similar manner but with much higher K_m values. The V_{max} values for catalysis of *O*-demethylation of DMXBA by this isozyme were also much less than for cytochrome 1A1.

In Vivo Biotransformation and Pharmacokinetics. When rats were orally administered 20 mg/kg DMXBA, all three hydroxy metabolites appeared to varying extents and then disappeared from the systemic circulation at slightly different rates (Fig. 2A). 4-OH-MBA was the dominant monohydroxy metabolite at the dose administered, followed by 2-OH-MBA and very small amounts of 2,4-DiOH-BA. However, in a small fraction (less than one third) of the male rats administered this dose, 2-OH-MBA was the most abundant hydroxy metabolite.

We then orally administered either 2-OH-MBA or 4-OH-MBA and determined their plasma levels over time (Fig. 2B). Despite their enhanced polarity, the time courses of absorption and elimination of these compounds were very similar to that of DMXBA (Fig. 2B). Their peak levels were similar to that of administered DMXBA.

The structures of the four compounds and the two pathways for DMXBA phase I biotransformation, derived from in vivo and in vitro data, are shown in Fig. 3. The pathway to 4-OH-MBA is the predominant means of phase I hepatic biotransformation, whereas the pathway on the right becomes more important with higher doses. It also is the pathway for formation of the dihydroxy metabolite 2,4-DiOH-BA.

Ionization of DMXBA and Its Metabolites. From the viewpoint of drug design, a complicating factor in the comparison of the relative binding affinities of these compounds was their variable state of ionization at pH 7.4 (Table 2). At this pH, the affinities of the two monohydroxy metabolites would be predicted to be much less than for DMXBA and 2,4-DiOH-BA, as determined from their lesser state of ionization. The imine N pK_a values of the two monohydroxy compounds were approximately 7.1, which is 0.5 pH units less than for the pK_a of 7.6 determined for DMXBA. Thus, at physiological pH, these metabolites would be only 32 or 33% ionized, whereas DMXBA would be 62% ionized. The determined pK_a values were used to predict the effective cationic concentrations of the four compounds for binding to the two nAChRs shown in Table 3. We consider these calculated cationic affinities to be the most useful estimates available for comparing the interactions of DMXBA and its phase I metabolites with the brain nAChRs.

Displacement of Radioligand Binding to Rat Brain Nicotinic Receptors. The relative abilities of the putative metabolites to interact with either rat brain $\alpha_4\beta_2$ or $\alpha7$ nicotinic receptors are shown in Table 3. Because cytisine binds preferentially to the desensitized form of the $\alpha_4\beta_2$ receptor, which routinely displays a several-hundred-fold higher affinity for ACh than the resting form, whereas BTX binds preferentially to the resting state of the $\alpha7$ receptor, these two sets of K_i values are not comparable with each other because they were not obtained from equivalent states of these two receptors.

TABLE 2
Ionization constants (pK_a) of DMXBA and its hydroxy metabolites determined by spectrophotometric titration in the presence of 150 mM NaCl
Standard errors are also indicated.

Compound	Imine Nitrogen pK_a	Ionized	Hydroxy Group pK_a
		%	
DMXBA	7.62 ± 0.03	62.4	None
4-OH-MBA	7.09 ± 0.04	33.0	9.50 ± 0.05
2-OH-MBA	7.07 ± 0.02	32.0	9.70 ± 0.05
2,4-DiOH-BA	7.41 ± 0.06	50.5	11.69 ± 0.07

[a] pH 7.4.

DMXBA competed with iodinated BTX (Fig. 4) for $\alpha7$ binding sites and with tritiated cytisine (data not shown) for predominantly $\alpha_4\beta_2$ receptor binding sites in rat brain in a manner consistent with competitive antagonism. The Scatchard plots for DMXBA inhibition of receptor binding by these two radioligands showed significant changes in slope but no significant changes in B_{max} values. The two monohydroxy metabolites inhibited the specific binding of both cytisine and BTX in a like manner (data not shown). The affinities of the four compounds for the $\alpha7$ receptor varied approximately 3-fold, with DMXBA showing the highest affinity for this nAChR subtype. When differences in ionization between compounds were accounted for, their affinities for this receptor varied less than 50%. Affinities for the $\alpha_4\beta_2$ receptor varied almost 4-fold, with 4-OH-MBA displaying the highest relative affinity. The predicted $\alpha_4\beta_2$ affinity of the

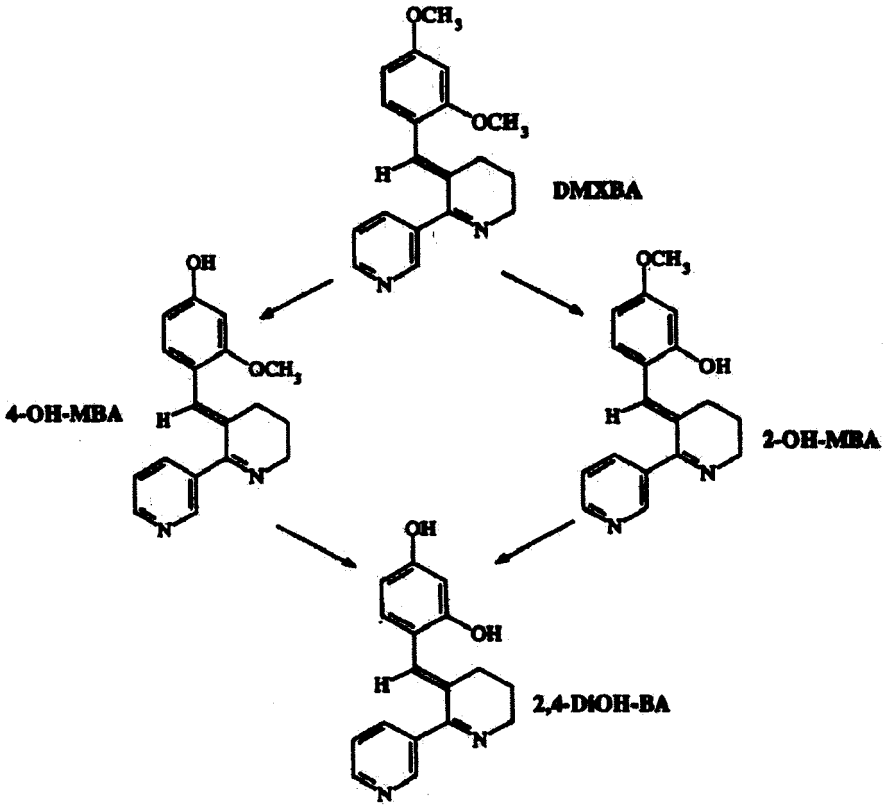

Fig. 3. Scheme showing the two major pathways for phase I biotransformation of DMXBA. The relative importance of the two potential pathways depends on DMXBA concentration at the sites of biotransformation as well as the concentrations and Michaelis-Menten kinetic properties of the cytochromes P450 involved in the two *O*-demethylations. The observed concentrations of the dihydroxy metabolite (2,4-DiOH-BA) were quite limited, both in vitro and in vivo, apparently because the two monohydroxylated metabolites are readily glucuronidated (Azuma et al., 1999).

TABLE 3

Inhibition of ^{125}I-BTX and [^{3}H]cytisine binding to rat brain membranes

The concentration of each radioligand was 1 nM. Each value represents the mean ± S.E.M. of values obtained from four (BTX) or three (cytisine) separate experiments. The K_i (Ion) values are inhibitory concentrations of the ionized form of the compound and were calculated assuming that only the cationic ionized form interacts with the ACh binding site. These values were calculated from the percentage ionization estimates at pH 7.4 shown in Table 2.

Compound	^{125}I-BTX Binding		[^{3}H]Cytisine Binding	
	K_i ± S.E.M.	K_i (Ion)	K_i ± S.E.M.	K_i (Ion)
		nM		
DMXBA	130 ± 14	81	253 ± 37	158
4-OH-MBA	235 ± 14	78	69 ± 30	23
2-OH-MBA	317 ± 67	105	387 ± 25	128
2,4-DiOH-BA	203 ± 5.0	102	206 ± 16	103

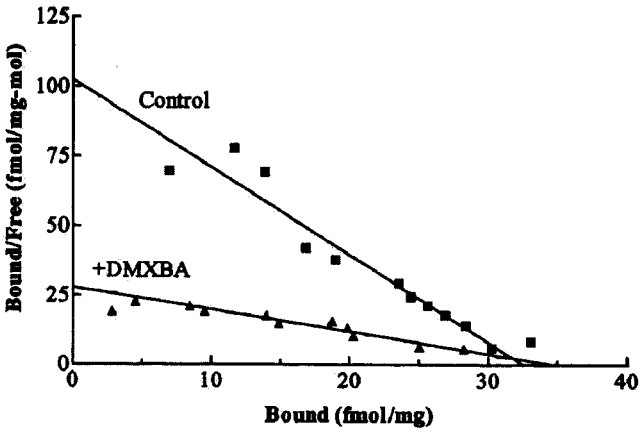

Fig. 4. DMXBA is a competitive inhibitor of specific binding of ^{125}I-BTX at rat brain α7 nicotinic receptors. The binding of this radiolabeled neurotoxin, measured alone and in the presence of DMXBA, is presented as a Scatchard plot. The mean K_d for ^{125}I-BTX binding, obtained from eight saturation experiments, was 0.32 ± 0.04 nM. Each saturation curve (data not shown) was fitted by a nonlinear least-squares method as described in the GraphPad Prism manual. The K_i calculated for DMXBA inhibition of iodinated BTX binding in these saturation experiments was 173 nM.

ionized form of 4-OH-MBA was approximately 6-fold greater than for DMXBA monocation.

The pH dependence (Fig. 5) of DMXBA displacement of BTX binding indicates that the ionized form of this ligand has much higher affinity for the α7 receptor than the un-ionized form. The observed pH dependence is interpreted as being largely caused by an effect on the ligand rather than on the receptor, because binding of BTX was unaltered over this pH range. Using one-way analysis of variance with the Tukey post test, the difference in the IC_{50} values calculated for the ionized form of DMXBA at pHs 6.6 and 7.4 was not statistically significant ($P > 0.05$); however, differences between the pH 7.4 and 8.2 estimates for ionized DMXBA were significant ($P < 0.05$). We suspect that there is a small pH effect on the receptor that causes a decrease in affinity for ionized DMXBA at the more alkaline pH levels, because we have observed an approximately 50% decrease in α7 receptor affinity for permanently ionized ACh, as measured by its displacement of iodinated BTX binding (LeFrancois and Kem, unpublished results). The actions of nicotine and ionizable ACh analogs on neuromuscular nAChRs have been shown previously to be primarily attributable to the ionized forms of

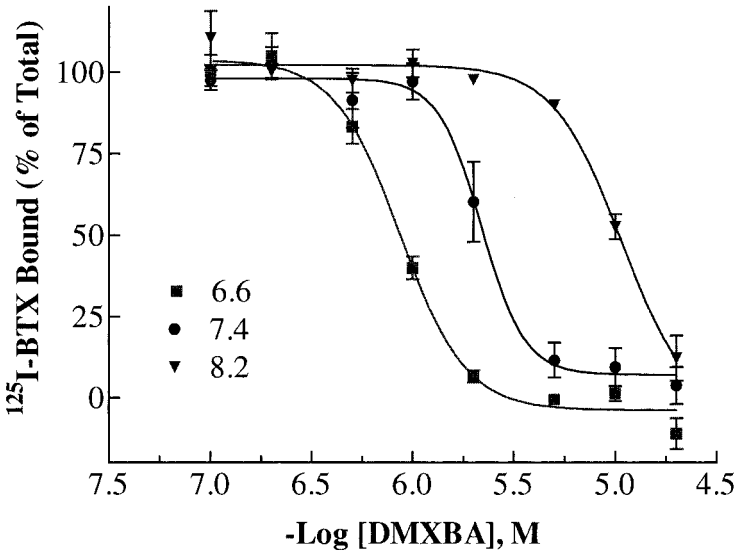

Fig. 5. pH dependence of DMXBA displacement of BTX at the rat brain α7 receptor ($n = 4$ for each curve). The saline used in this experiment contained 50 mM MOPS (pKa = 7.2), 1 mM $MgCl_2$, 120 mM NaCl, and 5 mM KCl. The pH values of the buffered salines were adjusted to 6.6, 7.4, and 8.2 by using small volumes of 1 N HCl or 1 N NaOH.

pH	IC_{50} (μM)	K_i (μM)	% Ionized	$K_{i\ Ionized}$ (μM)
6.6	1.02 ± 0.22	0.37 ± 0.06	91.3	0.34 ± 0.05
7.4	2.21 ± 0.30	0.80 ± 0.11	62.4	0.50 ± 0.07
8.2	10.19 ± 0.89	3.69 ± 0.32	20.8	0.77 ± 0.07

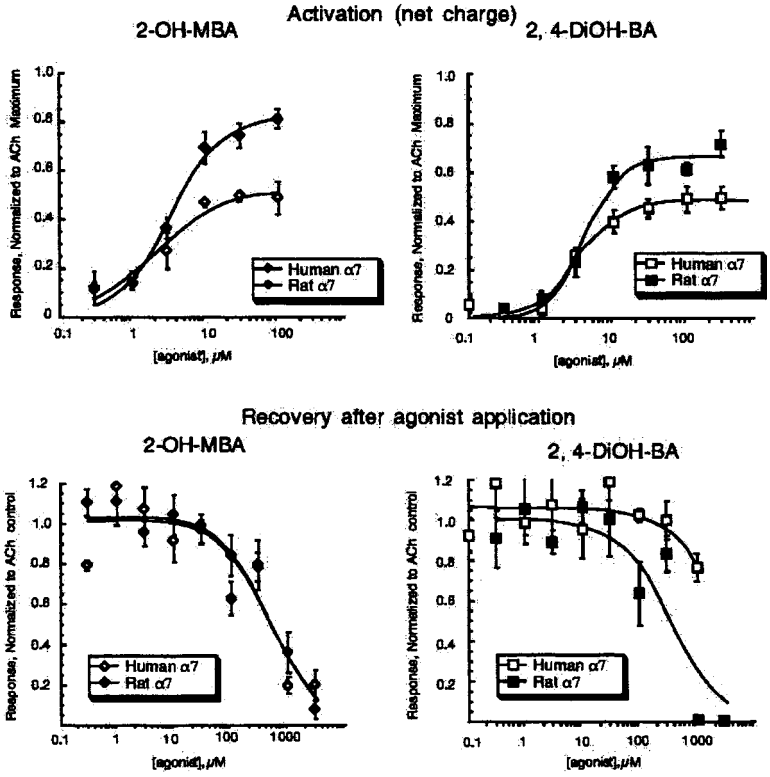

Fig. 6. Partial agonism of 2-OH-MBA and 2,4-DiOH-BA at rat and human α7 nicotinic receptors transiently expressed in the *X. laevis* oocyte. Each mean response is normalized with respect to the response to a 300-μM ACh control pulse administered 5 min preceding measurement of the test response. Bottom, the residual inhibition caused by these two DMXBA metabolites. To measure residual responsiveness of the receptor, the 300-μM ACh-stimulated current measured after 5-min washing away of the DMXBA compound was normalized to the initial response of the oocyte to the same concentration of ACh before DMXBA compound application. Each data point represents the mean ± S.E.M. of responses obtained from at least four oocytes.

these agonists (Barlow and Hamilton, 1962; Jeng and Cohen, 1980).

Physiological Effects of DMXBA and Its Metabolites on Brain nAChRs. Full concentration-response curves are shown for the agonist effects of the two new compounds, 2-OH-MBA and 2,4-DiOH-BA, on rat and human α7 nicotinic receptors (Fig. 6). The EC_{50} values for all four compounds show relatively minor differences (Table 4). It is interesting that all three DMXBA hydroxy metabolites exhibited efficacies that were consistently greater than that of DMXBA on α7 receptors from both mammalian species. Prior exposure of the receptors to a hydroxy metabolite also caused much less residual inhibition (reduced response to ACh 5 min after washing) in comparison with DMXBA. Whereas 100 μM DMXBA produced nearly 50% residual inhibition, the monohydroxy metabolites at this concentration displayed little residual inhibitory effect.

At the rat $\alpha_4\beta_2$ receptor, DMXBA was previously reported to have little (<3% of the maximal ACh current) or no agonistic action (de Fiebre et al., 1995). Similarly, we found that 0.3 and 3 μM concentrations of the four compounds caused barely measurable agonistic effects on human $\alpha_4\beta_2$ receptors (Fig. 7A). Exposure to these metabolites or DMXBA caused some residual inhibition, as measured after 5 min of washing the oocytes with saline (Fig. 7B). Their ability to inhibit the human $\alpha_4\beta_2$ receptor was also limited when 3 μM concentrations were coapplied with ACh (Fig. 8).

Partition Coefficients of DMXBA and Its Metabolites. The octanol/water partition coefficients of the compounds calculated by an atomic-fragment method predicted that a small decrease in lipid solubility would result from oxidative demethylation of one or more methoxy groups on the DMXBA benzylidene ring (Table 5). Although the experimental $P_{octanol/water}$ of DMXBA was in satisfactory agreement with the predicted value, the actual effect of demethylation on this partition coefficient was much greater than was predicted by this theoretical method.

The significant differences in the observed *P* values for the compounds were also reflected to some degree in the predicted Br:Bl concentration ratios of the compounds (Table 5); the ratio for DMXBA was the highest of the four compounds, and the ratio for the dihydroxy metabolite was the lowest.

TABLE 4

Relative potencies and efficacies of DMXBA and its hydroxy metabolites on human and rat α 7 nicotinic receptors expressed in *X. laevis* oocytes (standard errors are shown)

Numbers in parentheses are calculated EC_{50} values for just the ionized forms.

Compound	Rat Receptor		Human Receptor	
	EC_{50} (Ion)	Maximum Response	EC_{50} (Ion)	Maximum Response
	μM		μM	
DMXBA[a]	2.9 ± 0.08 (1.8)	0.59 ± 0.05	6.0 ± 2.4 (3.7)	0.23 ± 0.02
4-OH-MBA[a]	1.6 ± 0.02 (0.53)	0.77 ± 0.02	4.0 ± 0.8 (1.3)	0.44 ± 0.03
2-OH-MBA	3.3 ± 0.8 (1.1)	0.82 ± 0.06	2.1 ± 0.8 (0.67)	0.53 ± 0.05
2,4-DiOH-BA	3.9 ± 0.6 (2.0)	0.67 ± 0.03	3.2 ± 0.5 (1.6)	0.49 ± 0.02

[a] Data from Papke and Porter-Papke (2002).

Thus, oxidative demethylation is predicted to progressively decrease the ability of DMXBA metabolites to passively distribute to the central nervous system, the intended site of action. The experimental Br:Bl ratio for DMXBA was approximately 3.5, which was much higher than had been predicted, whereas the experimental ratios for the three hydroxy metabolites were all much lower than their predicted values. In general, the quantitative predictions were only in rough, qualitative agreement with our experimental brain/blood ratios.

All of the four compounds were predominantly bound to plasma proteins at low micromolar concentrations (Table 5). DMXBA was quite extensively bound (96%), followed by 2-OH-MBA (93%), 4-OH-MBA (83%), and finally 2,4-DiOH-BA (60%).

Molecular Conformations of DMXBA and Its Metabolites. The preferred conformations of the four compounds in their neutral and monocationic forms were very similar, derived from their semiempirical (PM5) quantum chemical models, as modeled in water using the COSMO approach. The preferred conformation of monoprotonated DMXBA is shown in the upper part of Table 6, which reports the predicted internitrogen distances and inter-ring angles for DMXBA in both its free base form and its more physiologically relevant monocationic form. In contrast with the preferred conformation of anabaseine (W. Kem, unpublished results) where the two rings are coplanar, in the preferred conformations of the four benzylidene compounds, the two anabaseinoid rings are twisted with respect to each other. Protonation of DMXBA further increases this angle. The preferred conformations of the three metabolites were not significantly different from those of DMXBA, except for a further twisting (approximately −40°) of the pyridyl ring with respect to the tetrahydropyridyl ring.

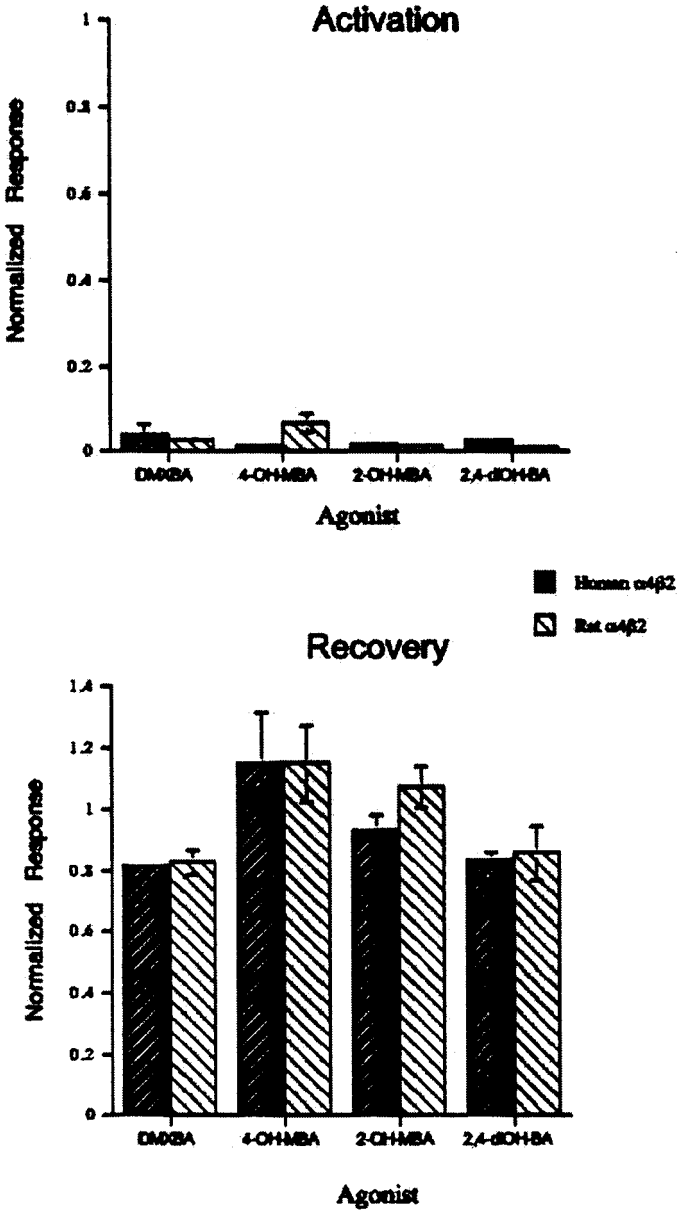

Fig. 7. Tests for agonistic activity of DMXBA and its three primary metabolites at rat and human $\alpha_4\beta_2$ nicotinic receptors transiently expressed in the *X. laevis* oocyte. Residual inhibition caused by DMXBA and its metabolites at this receptor subtype is also shown at the bottom. To measure residual responsiveness of the receptor, the 30-μM ACh-stimulated current measured after 5-min washing away of the DMXBA compound was normalized to the initial response of the oocyte to the same concentration of ACh before DMXBA compound application. Each data point represents the mean ± S.E.M. of responses obtained from at least four oocytes.

Discussion

O-Dealkylation is a commonly observed process in the biotransformation of drugs possessing such functional groups. We demonstrated the production of two demethylated monohydroxy DMXBA derivatives and small amounts of a dihydroxy product. Our efforts to produce a significant amount of

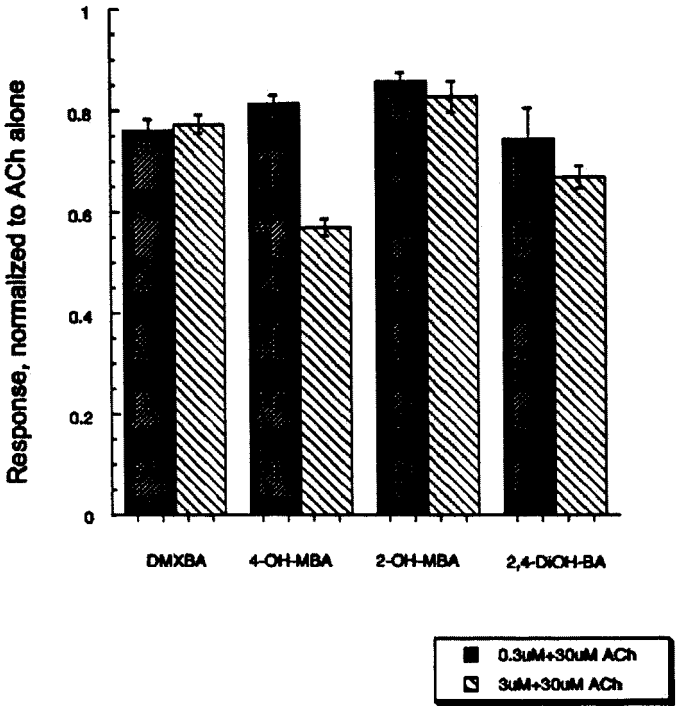

Fig. 8. Possible antagonistic activity of DMXBA and its hydroxy metabolites at human $\alpha_4\beta_2$ receptors expressed in the *X. laevis* oocyte. Oocytes were subjected to a simultaneous addition of the compound with a 30-μM ACh pulse, and the peak response was measured relative to that of the same ACh pulse alone. Two different concentrations (0.3 and 3 μM) of the DMXBA compound were tested. Each data bar represents the mean ± S.E.M. of responses obtained from at least four oocytes.

TABLE 5
Selected partitioning properties of DMXBA and its metabolites (standard errors are included)

Compound	$P_{octanol/water}$		Brain:Blood Concentration Ratio		Plasma Binding
	Predicted[a]	Experimental[b]	Predicted[c]	Experimental	
					% Free
DMXBA	1820	3810 ± 740	0.62	3.45 ± 0.57	4.1 ± 0.6
4-OH-MBA	616	246 ± 15	0.38	0.28 ± 0.03	17 ± 0.7
2-OH-MBA	616	75 ± 42	0.27	0.08 ± 0.01	7.2 ± 0.5
2,4-DiOH-BA	209	30 ± 14	0.16	<0.05	40 ± 4.5

[a] 1-Octanol/water partition coefficient, predicted by a group-fragment method (Viswanadhan et al., 1989).
[b] Experimental 1-octanol/water partition coefficient determined at pH 7.40 and then corrected for percentage ionization.
[c] Predicted from AM1 geometry-optimized structure (Brewster et al., 1996).

the dihydroxy metabolite in vitro by incubating microsomes with synthetic 4-OH-MBA were unsuccessful, and incubation with 2-OH-MBA yielded only small amounts. Apparently the OH substituent of 4-OH-MBA protects this initial metabolite from being *O*-demethylated at position 2, because 3-[(2-methoxy)benzylidene]anabaseine was readily *O*-demethylated (Table 1). The major cytochromes P450 catalyzing the two DMXBA demethylations (Fig. 3) in the rat are apparently different. This interpretation is consistent with the different storage stabilities of the two enzyme activities and with observed effects of selective cytochrome P450 inhibitors (Azuma et al., 1999; Kem et al., unpublished results).

A major difference between our biotransformation data and those of Azuma et al. (1999) pertained to 2-OH-MBA, which they did not detect in vitro or in vivo. However, they isolated its glucuronide from urine. They used a different pH and buffer system for their reversed-phase HPLC determinations, but we have found that their conditions would have resolved the 2-OH-MBA from the other metabolites. Most of their experiments used lower DMXBA concentrations, in which formation of 2-OH-MBA is less favored. Whereas 4-OH-MBA was usually the major in vivo metabolite of DMXBA in our experiments, we occasionally observed larger plasma concentrations of 2-OH-MBA in samples from certain rats. Significant variations in 4-OH-MBA plasma levels were also observed during phase I human tests (Kitagawa et al., 2003).

Hydroxy metabolite levels could be affected by their relative rates of conjugation and excretion, as well as their rates of production. It is known that 4-OH-MBA is readily glucuronidated (Azuma et al., 1999; Kitagawa et al., 2003; Kem et al., unpublished results). The plasma time profiles (Fig. 2B) of the orally administered monohydroxy metabolites were very similar to that of DMXBA (Fig. 2A). Thus, it seems that the rate of elimination of DMXBA and its metabolites from the plasma compartment is ultimately limited by some process subsequent to their phase I biotransformation.

The hydroxy metabolites displayed affinities similar to those of DMXBA for binding to rat brain $\alpha 7$ receptors as measured by the inhibition of [^{125}I]BTX binding. Because the ionized form of DMXBA displayed a much higher affinity for this receptor than the un-ionized form, we assume that the

TABLE 6
Minimum free-energy conformations in water predicted for DMXBA free base, DMXBA monocation, and monocationic forms of the three hydroxylated metabolites

Molecular modeling is described under *Materials and Methods*. The distances of heteroatoms and the dihedral angles in the different compounds are tabulated below the color-illustrated preferred conformation of the monocationic form of DMXBA. This structure is very similar to the solution conformation of 3-[(4-choloro)benzylidene]-anabaseine, which was based on NMR measurements (Zoltewicz et al., 1993).

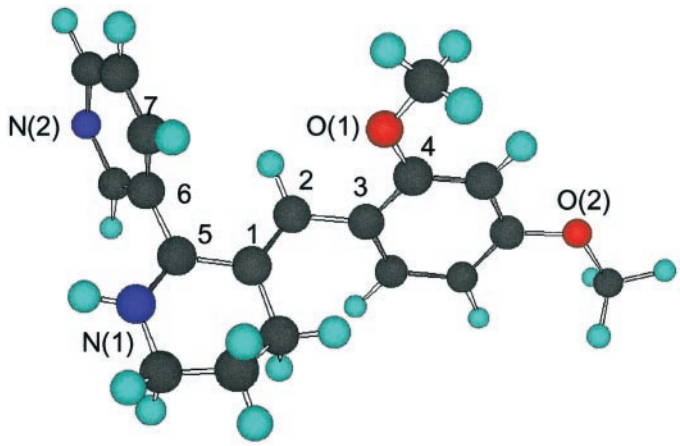

Compound	N(1)–N(2)	N(1)–O(1)	C(1)–C(2)–C(3)–C(4)	C(1)–C(5)–C(6)–C(7)
	Å	Å	°	°
DMXBA	4.27	5.57	107.4	−55.4
DMXBA(H^+)	4.43	6.38	−124.7	−81.4
2OH-MBA(H^+)	4.64	6.07	−126.8	−123.1
4OH-MBA(H^+)	4.63	5.85	−125.9	−121.2
2,4-DiOH-BA(H^+)	4.64	5.91	−129.3	−121.7

presence of a positive charge on the tetrahydropyridyl nitrogen is also very important for binding of the hydroxy metabolites. When the K_i values of the compounds are expressed in terms of their monocationic concentrations, one observes that the substitution of a hydroxy substituent for a methoxy substituent does not make a significant difference in binding affinity, at least for the rat form of this receptor.

A partial agonist activity at $\alpha 7$ receptors was reported previously for DMXBA (de Fiebre et al., 1995) and for its 4-OH-metabolite (Meyer et al., 1998). Here we show that the other two hydroxy metabolites also are partial agonists at this receptor. All three metabolites display greater efficacies than DMXBA on $\alpha 7$ receptors from both mammalian species. DMXBA is known to be approximately half as effective on the human $\alpha 7$ nicotinic receptor relative to the rat receptor (Briggs et al., 1997; Meyer et al., 1998). Here, we report that the efficacies of all the hydroxy metabolites are also less at the human $\alpha 7$ receptor compared with the rat receptor. Because the hydroxy compounds displayed binding affinities similar to those of DMXBA at the rat brain $\alpha 7$ receptor, hydroxylation effects on efficacy may be related more to increasing the ligand polarity than to formation of a specific hydrogen bond between the ligand and an amino acid side chain in the acetylcholine binding site of the receptor. The orientations of the benzylidene *ortho*-and *para*-hydroxy groups would be expected to be very different when the hydroxy metabolites are docked within the $\alpha 7$ receptor site. The basis for the lower apparent efficacy of DMXBA on the human $\alpha 7$ receptor is not yet known. DMXBA displays a much higher residual inhibitory activity than any of the hydroxy metabolites on this receptor. It binds to sites other than the ACh binding sites in the *Torpedo* muscle-type nAChR (Arias and Kem, unpublished results). Binding of DMXBA to allosteric sites on the $\alpha 7$ nAChR might contribute to its low efficacy and high residual inhibitory activity.

In a separate article (Machu et al., 2001), it was reported that all three hydroxy metabolites of DMXBA, but not DMXBA itself, are partial agonists at the mouse 5-HT_{3A} receptor, which is homologous with the nAChR $\alpha 7$ subunit. The 2-OH metabolite (EC_{50} = 2 μM) was most potent, and the 4-OH metabolite was least potent (EC_{50} = 17 μM). In contrast, these metabolites and DMXBA are antagonists at the human 5-HT_3 receptor (T. Machu and W. Kem, in preparation). Experiments are in progress to identify amino acid side chains within this serotonin receptor that determine efficacies of these benzylidene anabaseines. The calculated conformations of the four benzylidene-anabaseine compounds (Table 6) will be useful in computer docking these ligands with ACh and 5-HT_3 receptor models. DMXBA and 4-OH-BA bind to the acetylcholine binding protein (Smit et al., 2001), a soluble protein homologous with the extracellular domain of nicotinic receptors with known crystal structure, with high affinities very similar to what we report here for the rat $\alpha 7$ receptor (Smit and Kem, unpublished results).

All three hydroxy metabolites acted as antagonists during electrophysiological experiments with $\alpha 4\beta 2$ receptors expressed in the *X. laevis* oocyte but only at relatively high concentrations (>3 μM) that are unlikely to have been attained in previously published behavioral experiments, which did not exceed a 10-mg/kg dose (Kem, 2000). In Fig. 2A, the highest DMXBA plasma level attained by a 20-mg/kg dose was approximately 300 ng/ml (0.79 μM). Assuming that peak concentrations are proportional to the dose (Azuma et al., 1999), then a 10-mg/kg oral dose would be predicted to cause a peak plasma concentration of approximately 0.4 μM. Because plasma binding of DMXBA is very high (96% in Table 5), the maximum free concentration of DMXBA attained in vivo (0.016 μM) would have been much lower than the concentrations tested for inhibition of $\alpha_4\beta_2$ receptor function in our *X. laevis* oocyte experiments (Fig. 8). Although 4-OH-MBA displayed less plasma protein binding, it also attained a much lower plasma concentration after DMXBA administration. A recent study reported that DMXBA inhibition of $\alpha_4\beta_2$ receptors expressed in human embryonic kidney 293 cells occurred with a high IC_{50} of 10 μM (Michelmore et al., 2002). Thus, the extent of DMXBA inhibition of this particular receptor in the published rat behavior studies was probably limited (Kem, 2000).

A chemical property of great relevance for drug design is the ability of a molecule to partition into a lipid phase such as a cell membrane. We determined with great care the $P_{\text{octanol/water}}$ values of these compounds (Table 5). Our P value for DMXBA was much greater than a value that we obtained initially using a less reliable spectrophotometric method (Mahnir et al., 1998). The large P value for DMXBA indicates that its un-ionized form is highly lipophilic. A high P value for DMXBA was predicted by an algorithm derived from the AM1 geometry-optimized structure, which also predicted that the hydroxy metabolites would have significantly reduced P values relative to DMXBA.

Because several algorithms have been published for predicting steady-state Br:Bl concentration ratios, we measured brain and blood concentrations for each compound resulting from four intraperitoneal injections over a 6-h time interval (Table 5). Whereas DMXBA accumulated in whole brain to a much greater extent than was predicted, the hydroxy metabolites accumulated in the brain to a much lesser extent than was predicted. The Br:Bl ratio of 4-OH-MBA, which accumulated more than the others, was still less than 10% of the DMXBA ratio, whereas the ratio for 2-OH-MBA was approximately 50 times less than for DMXBA. For 2,4-DiOH-BA, it was only possible to estimate the upper limit of this ratio because this compound could not be detected in the brain. The Br:Bl predictions for the two compounds displaying the most extreme solubility characteristics, namely DMXBA (most lipophilic) and 2,4-DiOH-BA (most hydrophilic), were not very satisfactory. The predicted as well as measured Br:Bl ratios refer to total (bound plus free) brain and blood concentrations of the compounds. The relationship between the bound and free concentrations of a compound may vary with the compartment, making successful predictions difficult.

The poor penetration of the hydroxy metabolites into the brain cannot be caused by differences in binding to plasma proteins. We measured this binding (Table 5) and found that progressive hydroxylation actually decreased plasma protein binding, which would increase the proportion of these molecules available for passive diffusion into the brain. Differing degrees of ionization also cannot explain the different Br:Bl ratios, because the lower pK_a values of the monohydroxy metabolites would actually favor their entry into the brain. A more likely explanation is that, because of their greater H-bonding propensities, these metabolites are unable to readily enter the brain by passive diffusion. Further experiments are required to determine the relative permeabilities of the compounds for entry into

the brain and to assess whether the *p*-glycoprotein–mediated transporter system also influences their brain entry.

Because the metabolites are more effective than DMXBA and in some cases more likely to bind to the human-type receptor, it seemed possible that some of the stimulatory effects of orally administered DMXBA might be caused by these compounds. Taken from the Br:Bl ratios reported in Table 5, the three metabolites apparently differ greatly in their relative brain uptakes. Thus, the higher efficacies of the monohydroxy compounds may not enhance the response of whole animals to DMXBA because these compounds display poor penetration into the brain and are present in the plasma at significantly lower levels than DMXBA. This would be consistent with the lower (approximately 3-fold) potency of 4-OH-MBA relative to DMXBA reported in whole animal experiments (Kasahara et al., 1998; Buccafusco and Terry, 2000; Woodruff-Pak et al., unpublished results). Further studies of the brain and plasma levels of DMXBA and its metabolites are warranted because metabolite brain levels may change during long-term administration (Ghosheh et al., 2001).

Acknowledgments

We thank Dr. C. K. Tu for assistance in computer estimations of the microsome enzyme properties and the compound pK_a values. We thank M. Garcia for the rat jugular vein cannulations.

References

Arendash GW, Sengstock GJ, Sanberg PR, and Kem WR (1995) Improved learning and memory in aged rats with chronic administration of the nicotinic receptor agonist GTS-21. *Brain Res* **674:**252–259.

Azuma R, Komuro M, Korsch BH, Andre JC, Onnagawa O, Black SR, and Mathews JM (1999) Metabolism and disposition of GTS-21, a novel drug for Alzheimer's disease. *Xenobiotica* **29:**747–762.

Azuma R, Minami Y, and Satoh T (1996) Simultaneous determination of GTS-21 and its metabolite in rat plasma by high-performance liquid chromatography using solid-phase extraction. *J Chromatogr B* **686:**229–234.

Barlow RE and Hamilton JT (1962) Effects of pH on the activity of nicotine and nicotine monomethiodide on the rat diaphragm preparation. *Br J Pharmacol* **18:**543–549.

Brewster ME, Pop E, Huang M-J, and Bodor N (1996) AM1-based model system for estimation of brain/blood concentration ratios. *Int J Quantum Chem Quantum Biol Symp* **23:**51–63.

Briggs CA, Anderson DJ, Brioni JD, Buccafusco JJ, Buckley MJ, Campbell JE, Decker MW, Donnelly-Roberts D, Elliott RL, Gopalakrishan M, et al. (1997) Functional characterization of the novel neuronal nicotinic acetylcholine receptor ligand GTS-21 *in vitro* and *in vivo. Pharmacol Biochem Behav* **57:**231–241.

Buccafusco JJ and Terry AV Jr (2000) Multiple central nervous system targets for eliciting beneficial effects on memory and cognition. *J Pharmacol Exp Ther* **295:** 438–446.

Champtiaux N, Han ZY, Bessis A, Rossi FM, Zoli M, Marubio L, McIntosh JM, and Changeux JP (2002) Distribution and pharmacology of alpha6-containing nicotinic acetylcholine receptors analyzed with mutant mice. *J Neurosci* **22:**1208–12017.

de Fiebre CM, Meyer EM, Henry JC, Muraskin SI, Kem WR, and Papke RL (1995) Characterization of a series of anabaseine-derived compounds reveals that the 3-(4)-dimethylaminocinnamylidine derivative (DMAC) is a selective agonist at neuronal nicotinic alpha7 ^{125}I alpha-bungarotoxin receptor subtypes. *Mol Pharmacol* **47:**164–171.

Dajas-Bailador FA, Soliakov L, and Wonnacott S (2002) Nicotine activates the extracellular signal-regulated kinase 1/2 via the alpha7 nicotinic acetylcholine receptor and protein kinase A, in SH-SY5Y cells and hippocampal neurons. *J Neurochem* **80:**520–530.

Dineley KT, Bell KA, Bui D, and Sweatt JD (2002) Beta-amyloid peptide activates alpha7 nicotinic acetylcholine receptors expressed in *Xenopus* oocytes. *J Biol Chem* **277:**25056–25061.

Flores CM, Rogers SW, Pabreza LA, Wolfe BB, and Kellar KL (1992) A subtype of nicotinic cholinergic receptor in rat brain is composed of α4 and β2 subunits and is up-regulated by chronic nicotine treatment. *Mol Pharmacol* **41:**31–37.

Freedman R, Adler LE, Waldo M, Myles-Worsley M, Nagamoto HT, Miller C, Kisly M, McRae K, and Cawthra E (1996) Inhibitory gating of an evoked response to repeated auditory stimuli in schizophrenic and normal subjects: human recordings, computer simulation and an animal model. *Arch Gen Psychiatry* **53:**1114–1121.

Gibaldi M and Perrier D (1982) *Pharmacokinetics,* Marcel Dekker, New York.

Ghosheh OA, Dwoskin LP, Miller DK, and Crooks PA (2001) Accumulation of nicotine and its metabolites in rat brain after intermittent or continuous peripheral administration of [2′-^{14}C]nicotine. *Drug Metab Dispos* **29:**645–651.

James MO and Little PJ (1983) Modification of benzo(a)pyrene metabolism in hepatic microsomes from untreated and induced rats by imidazole derivatives which inhibit monooxygenase activity and enhance epoxide hydrolase activity. *Drug Metab Dispos* **11:**350–354.

Jeng AY and Cohen JB (1980) Agonists of *Torpedo* nicotinic receptors: essential role of a positive charge. *Ann NY Acad Sci* **358:**370–373.

Kasahara N, Azuma R, Yamamoto J, and Matsuura N (1998) Mnemonic effects of GTS-21 and its 4-OH metabolite on scopolamine-induced deficits in passive avoidance behavior in the rat (Abstract). *Neurobiol Aging* **19(Suppl):**182.

Kem WR (1971) A study of the occurrence of anabaseine in *Paranemertes* and other nemertines. *Toxicon* **9:**23–32.

Kem WR (2000) The brain alpha7 nicotinic receptor may be an important therapeutic target for the treatment of Alzheimer's disease: studies with DMXBA (GTS-21). *Behav Brain Res* **113:**169–183.

Kem WR, Mahnir VM, Papke R, and Lingle C (1997) Anabaseine is a potent agonist upon muscle and neuronal alpha-bungarotoxin sensitive nicotinic receptors. *J Pharmacol Exp Ther* **283:**979–992.

Kihara T, Shimohama S, Sawada H, Honda K, Nakamizo T, Shibasaki H, Kume T, and Akaike A (2001) Alpha7 nicotinic receptor transduces signals to phosphatidylinositol-3-kinase to block a B-amyloid –induced neurotoxicity. *J Biol Chem* **276:**13541–13546.

Kihara T, Shimohama S, Sawada H, Kimura J, Kume T, Kochiyama H, Maeda T, and Akaike A (1997) Nicotinic receptor stimulation protects neurons against B-amyloid toxicity. *Ann Neurol* **42:**159–163.

Kitagawa H, Takenouchi T, Azuma R, Wesnes KA, Kramer WG, Clody DE, and Burnett AL (2003) Safety, pharmacokinetics and effects on cognitive function of multiple doses of GTS-21 in healthy, male volunteers. *Neuropsychopharmacology* **28:**542–551.

Klamt A and Shuurmann G (1993) COSMO—a new approach to dielectric screening in solvents with explicit expressions for the screening energy and its gradient. *J Chem Soc Perkin Trans II* **1995:**799–805.

Lindstrom J (1996) Neuronal nicotinic acetylcholine receptors, in *Ion Channels* (Narahashi T ed) pp 377–450, Plenum Press, New York.

Machu TM, Hamilton ME, Field TR, Shanklin CL, Harris MC, Sun H, Henner TE Jr, Soti F, and Kem WR (2001) Benzylidene analogs of anabaseine display partial agonist and antagonist properties at the mouse 5-hydroxytryptamine3A receptor. *J Pharmacol Exp Ther* **299:**1112–1119.

Mahnir VM, Lin B, Prokai-Tatrai K, and Kem WR (1998) Pharmacokinetics and urinary excretion of DMXBA (GTS-21), a compound enhancing cognition. *Biopharm Drug Dispos* **19:**147–151.

Marks MJ and Collins AC (1982) Characterization of nicotine binding in mouse brain and comparison with the binding of alpha-bungarotoxin and quinuclidinyl benzylate. *Mol Pharmacol* **22:**554–564.

Martin EJ, Panikar KS, King MA, Deyrup M, Hunter B, Wang G, and Meyer EM (1994) Cytoprotective actions of 2, 4-dimethoxybenzylidene anabaseine in differentiated PC12 cells and septal cholinergic cells. *Drug Dev Res* **31:**134–141.

Martin-Ruiz CM, Court JA, Molnar E, Lee M, Gotti C, Mamalaki A, Tsouloufis T, Tzartos S, Ballard C, Perry RH, et al. (1999) Alpha4 but not alpha3 and alpha7 nicotinic acetylcholine receptor subunits are lost from the temporal cortex in Alzheimer's disease. *J Neurochem* **73:**1635–1640.

Matuszewski BK, Constanzer ML, Woolf EJ, Au T, and Haddix H (1994) Determination of MK-507, a novel topically effective carbonic anhydrase inhibitor, and its de-ethylated metabolite in human whole blood, plasma and urine by high-performance liquid chromatography. *J Chromatogr B* **653:**77–85.

Meyer EM, Tay ET, Zoltewicz JA, Meyers C, King MA, Papke RL, and de Fiebre CM (1998) Analysis of 3-[(4-hydroxy, 2-methoxy)benzylidene]anabaseine selectivity and activity at human and rat alpha7 nicotinic receptors. *J Pharmacol Exp Ther* **287:**918–925.

Michelmore S, Croskery K, Nozulak J, Hoyer D, Longato R, Weber A, Bouhelal R, and Feuerbach D (2002) Study of the calcium dynamics of the human alpha4-beta2 and alpha7 nicotinic receptors. *Naunyn Schmiedebergs Arch Pharmacol* **366:**235–245.

Papke RL and Porter-Papke J (2002) Comparative pharmacology of rat and human alpha7 nAChR conducted with net charge analysis. *Br J Pharmacol* **137:**49–61.

Sabbagh MN, Reid RT, Corey-Bloom J, Rao TS, Hansen LA, Alford M, Masliah E, Adem A, Lloyd GK, and Thal LJ (1998) Correlation of nicotinic binding with neurochemical markers in Alzheimer's disease. *J Neural Transm* **105:**709–717.

Shimohama S, Greenwald DL, Shafron DH, Akaika A, Maeda T, Kaneko S, Kimura J, Simpkins CE, Day AL, and Meyer EM (1998) Nicotinic alpha 7 receptors protect against glutamate toxicity and neuronal ischemic damage. *Brain Res* **779:**359–363.

Smit AB, Syed N, Schaap D, van Minnen J, Klkumperman J, Kits KS, Lodder H, van der Schors RC, van Elk R, Sorgedrager B, et al. (2001) A glia-derived acetylcholine-binding protein that modulates synaptic transmission. *Nature (Lond)* **411:**261–268.

Stevens KE, Kem WR, Mahnir VM, and Freedman R (1998) Selective alpha7-nicotinic agonists normalize inhibition of auditory response in DBA mice. *Psychopharmacology (Berl)* **136:**320–327.

Viswanadhan VN, Ghose AK, Revankar GR, and Robins RK (1989) Atomic physicochemical parameters for 3 dimensional structure directed quantitative structure-activity relationships. 4. Additional parameters for hydrophobic and dispersive interactions and their application for an automated superposition of certain naturally-occurring nucleoside antibiotics. *J Chem Inf Comput Sci* **29:**163–172.

Wang H-Y, Lee DHS, Davis CB, and Shank RP (2000) Amyloid peptide AB1–42 binds selectively and with picomolar affinity to alpha7 nicotinic receptors. *J Neurochem* **75:**1155–1161.

Woodruff-Pak DS, Li Y-T, and Kem WR (1994) A nicotinic receptor agonist (GTS-21), eyeblink classical conditioning, and nicotinic receptor binding in rabbit brain. *Brain Res* **645:**309–317.

Zoltewicz JA, Prokai-Tatrai K, Bloom LB, and Kem WR (1993) Long range transmission of polar effects in cholinergic 3-arylidene anabaseines. Conformations calculated by molecular modelling. *Heterocycles* **35:**171–179.

Address correspondence to: Dr. William R. Kem, Department of Pharmacology and Therapeutics, College of Medicine, University of Florida, Gainesville, FL 32610-0267. E-mail: kem@pharmacology.ufl.edu